Besides stem canker severity, oilseed rape host genotype matters for the production of Leptosphaeria maculans fruit bodies

Lydia Bousset, Patrick Vallée, Régine Delourme, Nicolas Parisey, Marcellino Palerme, Melen Leclerc

Besides stem canker severity, oilseed rape host genotype matters for the production of *Leptosphaeria maculans* fruit bodies

Lydia Bousset*, Patrick Vallée, Régine Delourme, Nicolas Parisey, Marcellino Palerme, Melen Leclerc

INRAE, UMR1349 IGEPP, F-35653 Le Rheu, France
*Email: lydia.bousset @inrae.fr, Phone: +33 2 23 48 51 85, Fax: +33 2 23 48 51 50

Total word count:

- main body of the text: 4875 words
- Introduction: 995
- Materials and Methods: 1590
- Results: 722
- Discussion: 1596

With 8 Figures and 3 Tables (2 with colours)
Supporting information with 14 Figures and 13 Tables (2 with colours)

Abstract

For fungal cyclic epidemics on annual crops, the pathogen carry-over is an important but poorly documented step. Plant resistance affects the pathogen development within the epidemics but we lack data on the inter-annual transmission of inoculum. For *Leptosphaeria maculans* on 15 oilseed rape genotypes in field during 4 growing seasons, stem canker severity was visually scored at harvest. The number of fruit bodies produced on incubated stubble was quantified using an automated image

analysis framework. Our results confirm that fruit body production increases with disease severity and is significantly affected by host genotype and nitrogen supply. Tracking individual stems through incubation, we confirm for the first time that the oilseed rape genotype has a direct effect on inoculum production, not only disease severity. This major effect of genotype on inoculum carry-over should be taken into account in models of varietal deployment strategies.

Keywords: blackleg, disease phenotyping, epidemiology, image analysis, inoculum potential, transmission

Introduction

A key development in disease control has been the breeding and deployment of crop varieties with genetically controlled resistance to pathogens, but most pathogens have repeatedly evolved and overcome qualitative resistance genes (Burdon *et al*. 2016). Therefore, a critical challenge is to design and implement durable crop protection strategies against rapidly evolving pathogens (Cowger & Brown 2019). Any mitigation strategy that reduces the transfer of inoculum between seasons, therefore the effective size of pathogen populations, should limit the evolutionary potential of pathogens, and increase resistance durability (Bousset & Chèvre 2013; Zhan *et al*. 2015). In experiments, combining quantitative with qualitative resistance (Brun *et al*. 2010: Delourme *et al*. 2014; Lasserre-Zuber *et al*. 2018), burying stubble to reduce inoculum transmission (Daverdin *et al*. 2012), or removing leaf litter in combination with reduced fungicide application (Didelot *et al*. 2016) has delayed adaptation. In models and experiments, the spatio-temporal distribution of host resistance in cultivated landscapes was optimised to mitigate disease transmission (Lô-Pelzer *et al*. 2010; Bousset *et al*. 2018; Papaïx *et al*. 2018; Rimbaud *et al*. 2018; Watkinson-Powell *et al*. 2019). However, model validation and accurate predictions rely on the availability of data that are difficult and costly to collect at these large scales.

On annual crops, many plant diseases have cyclic epidemics (Zadoks & Schein 1979; Bousset & Chèvre 2013; Fig. 1A). Their dynamics are highly influenced by both temporal and spatial discontinuities, induced by the climate (e.g. seasonality) or by human actions (e.g. sowing and harvesting). At the beginning of the cropping season, the primary inoculum level is a product of carry-over from the prior crop(s) and/or dispersal. Mitigation strategies can thus target this carry-over of the pathogen using resistant varieties (Marcroft *et al*. 2004a), biocontrol agents (Bailey *et al*. 2004), or preventive management of crop residues (Wherrett *et al*. 2003). However, inoculum survival and transmission are difficult to estimate in field and predict (Bailey *et al*. 2004; Bousset *et al*. 2015).

Host resistance impacts pathogen life history traits during the epidemic phase (e.g. infection efficiency, latent period or sporulation) (Bruns *et al*. 2012; Delmas *et al*. 2016; Dumartinet *et al*. 2020; Leclerc *et al*. 2019; Bove & Rossi 2020). Qualitative host resistance reduces the number of compatible infections whereas quantitative host resistance reduces the amplification during the epidemics (Fig. 1B). In addition, the selective deployment of resistant host genotypes can reduce landscape connectivity following the intercrop (Lô-Pelzer *et al*. 2010; Bousset & Chèvre 2013; Papaïx *et al*. 2018; Rimbaud *et al*. 2018; Watkinson-Powell *et al*. 2019). Little is known about the direct effect of quantitative host resistance on initial amount of inoculum at the beginning of the next cropping season (i.e. inter-annual transmission, Fig. 1B). Quantitative resistance affects transmission in *Phytophthora infestans* through a trade-off between crop infection and survival on tubers (Pasco *et al*. 2016). A trade off was detected in *Zymoseptoria tritici*, but varietal effects were not investigated (Suffert *et al*. 2018a). In downy mildew, the effect of quantitative resistance was assessed on oospore production (inoculum for inter-annual transmission; Delbac *et al*. 2019).

Inoculum transmission between seasons was described in *Leptosphaeria maculans* on winter oilseed rape sown in autumn. This fungal pathogen initiates epidemics early in the cropping season (in autumn) with stubble-borne ascospores that can spread between fields across the landscape (West *et al*. 2001). It produces Phoma leaf spots on host leaves that are observed between autumn and early spring. Then, stem cankers develop from spring to summer, up to the time of harvest, following

78 systemic growth of fungal hyphae from leaf spots to the leaf petiole through xylem vessels, and
79 subsequently to the stem base. The fungus can survive as hyphae in crop stubble, more specifically
80 in stems around crown level, forming two kinds of fruit bodies: pycnidia and pseudothecia.
81 Pseudothecia can only be formed following sexual reproduction if isolates of opposite mating types
82 co-occur in the same oilseed rape stem. Infected stubble ensures the carry-over of the fungus from
83 one cropping season to the next and serves as the main source of inoculum.

84 For *L. maculans*, several studies have shown that the number of produced pseudothecia, that
85 release initial inoculum ascospores, was correlated with Phoma stem canker severity (McGee &
86 Emmett 1977; Marcroft *et al*. 2004a; Lô-Pelzer *et al*. 2009) and that some quantitative host resistances
87 tends to decrease severity at harvest (Marcroft *et al*. 2004b; Lô-Pelzer *et al*. 2009). Host genotype
88 can significantly affect both the visual density of pseudothecia, and the number of released ascospores
89 (Marcroft *et al*. 2004b). However, properly disentangling the effects of host genotype on stem canker
90 severity and fruit body production remains to be achieved. Therefore, the question of a direct genetic
91 effect on the production of fruit bodies, and thus temporal transmission of inoculum between seasons,
92 is still unknown for this pathosystem. The development of high-precision and high-throughput
93 phenotyping methods could improve experimental quantification of plant pathogens, alleviate the
94 tedious manual quantification of fruit bodies on many genotypes, and improve knowledge and data
95 on pathogen carry-over. Imaging and processing algorithms to segment and count regions,
96 circumvented the long and tedious manual counting (Stewart *et al*. 2016; Karisto *et al*. 2018; Yang &
97 Hong 2018) and were applied to the automated quantification of fruit bodies of *L. maculans* (Bousset
98 *et al*. 2019). This offers a means to overcome the experimental bottleneck and assess the effect of
99 host quantitative resistance on pathogen carry-over.

100 In this study, we address the effect of host resistance on the carry-over of inoculum between
101 consecutive years, to understand how host genotype might affect fruit body production and the effects
102 of a common cropping practice, i.e. nitrogen fertilization, and disease severity at harvest in the
103 preceding growing season (year). We consider *L. maculans* on oilseed rape as an example

104 pathosystem and use an imaged-based phenotyping method for quantifying fruit bodies that appeared
105 on diseased stems collected in experimental field plots, after an incubation period. We analyse the
106 main drivers of this poorly known life-history trait of the pathogen.
107
108 **Materials and methods**
109 *Experimental fields and contamination of field plots*
110 This experiment was run on the INRAE UE La Motte experimental station located in Le Rheu
111 (48.1°N, 1.5°W), in Brittany, France. Winter *B. napus* genotypes were grown in 5-row plots (2.5 m^2)
112 and assessed for stem canker (details are given in Table S1.1). The cropping season extends from
113 sowing in autumn to harvest the following summer and was repeated in the 4 years named 12-13, 13-
114 14, 14-15 and 15-16. We followed the same 15 genotypes in years 12-13, 13-14 and 14-15, (Table 1;
115 S1.2) and six genotypes were added in year 15-16 (Table 1). The varieties were chosen to represent a
116 wide range of winter oilseed rape diversity and derived from different breeding programs.
117 In the four years, nitrogen supply was normal (Nh) according to usual practices in
118 conventional cultivation to achieve yield potential of modern winter oilseed rape varieties (Bouchet
119 et al. 2014) (Table S1.3). In years 14-15 and 15-16, the panel was replicated with low (Nl) nitrogen
120 availability. On these Nl plots, no organic matter was spread on the fields for 3 years before the trials
121 and the previous crops were grown under a low input management system. This limited the amount
122 of mineral N in soil in the experimental plots, avoiding organic matter mineralisation into nitrogen
123 later available to the plants.
124 Homogeneous disease infection was achieved with contaminated stems collected from the
125 previous year on the susceptible Bristol and miscellaneous varieties. In the experimental area and
126 around Phoma stem cankered stubble, only *L. maculans* leaf spots were observed which supported
127 the hypothesis of the very small prevalence of the other causal agent *L. biglobosa* in this area (Bousset
128 et al. 2019). Stems were scattered throughout the plots in each cropping season at a density of two
129 stems per m^2 when the crop was at the two to three leaf growth stage. Each variety was grown on

three replicated plots, from which stems were pooled for the current analysis. Sprinklers were run twice per day (4 mm per day) from plant emergence to the appearance of first leaf spots to promote fruit body maturation and spore release. This kept the time from spreading the contaminated stems to the appearance of leaf spots similar over years (Fig. S1E). No fungicides were applied throughout the season. Phoma stem canker severity was assessed 2-3 weeks before crop maturity on a 1 to 6 scale as follows: S1 = no disease, S2a = 1-5%, S2b – 6-25%, S3 = 26-50%, S4 = 51-75%, S5 = 76-99%, S6= 100% of crown cross section with Phoma stem canker symptoms. Severity classes 2a and 2b were distinct for the analysis of fruit body formation on stems, but pooled before the calculation of plot canker severity. The G2 aggregated disease index was calculated as follows (Aubertot et al. 2004):

$$G2 = (0 \times n_1 + 1 \times n_2 + 3 \times n_3 + 5 \times n_4 + 7 \times n_5 + 9 \times n_6)/N$$

with n_i being the number of stems in severity class S_i , respectively and N the total number of stems.

The climate of the experimental area is oceanic. Meteorological data were obtained from the INRAE CLIMATIK database, for Le Rheu weather station, on an hourly basis. Cumulative temperature (Fig. S1ab), rainfall (Fig. S1cd), and number of days that are favourable for pseudothecia maturation (Fig. S1e) were calculated from start (shortly after harvest in June; Table S1.1) to end of incubation when stems were retrieved from the field (at the end of the following winter; Table S1.1). A day was considered favourable if the mean temperature was between 2 and 20°C and if the cumulative rainfall over the previous 11 days before (including the day in question) exceeded 4 mm (Aubertot *et al*. 2006; Lô-Pelzer *et al*. 2009). Given these parameter values, 64 favourable days were required for 50% of pseudothecia to reach maturation. We were able to compare the number of calendar days needed to reach maturation in different years (Fig. S1E).

Stubble incubation to promote fruit body formation

Phoma stem canker severity was assessed at harvest, and then tracked for each individual stem piece comprising the crown and upper 10 cm (Bousset *et al.* 2019). The sampling was constrained by the availability of diseased stems across severity classes. After pooling the three replicated plots of

each variety, 30 stems in each of the 6 severity classes were randomly selected. If fewer than 30 stems (per class) were available, then all were kept. Within each variety and severity class, groups of 5 stem pieces attached together on BBQ sticks were labelled with a barcode (Bousset *et al.* 2019).

The selected stem pieces were incubated in field conditions at INRAE Le Rheu. Over summer, they were placed on a 1:1:1 mix of sand, peat and compost spread on the ground to avoid weed emergence, then transferred in autumn in experimental plots of winter oilseed rape to mimic incubation under the following season's crop and to allow detection of released spores. Complete maturation was indicated by the end of the appearance of new leaf spots on susceptible plants around the incubating stem pieces. The stem pieces were recollected, washed, dried and stored (Table 1). All stem pieces from a given year were incubated in the same time and location, starting in the summer following harvest.

Image acquisition, processing and post-processing

The fruit bodies appeared on diseased stem pieces were quantified using image-based phenotyping settings described in Bousset *et al.* (2019). In short, a picture of each group of 5 dry stems was taken with the barcoded label, placed on a glass plate, 16 cm above a blue background (PVC sheet Lastolite Colormatt electric blue). Two FotoQuantum LightPro 50 × 70cm softboxes were placed on both sides of the stem pieces with 4 daylight bulbs each (5400K, 30W) within the lower 45° angle. Pictures were taken with a Nikon D5200 with an AF-S DX Micro Nikkor 40mm 1:2.8G lens, on a Kaiser Repro stand, with a wired remote control. Aperture was set at F22 for maximal depth of field, iso 125, daylight white balance. Pictures were saved as RGB images with a resolution of 6000 × 4000 pixels.

Pictures were pre-processed by reading the barcode to rename the files, splitting each digital image in several new images, each containing only one stem segmented with an unsupervised method. Finally, each new image was cropped to keep only the 5 cm portion on the crown end of the stem, i.e. where pseudothecia are mainly located.

Then, stem pixels were classified either in state F (fruit bodies) or in state S (stem) using a supervised machine learning algorithm. We did not re-train the algorithm for processing our images, because learning and testing data used by Bousset et al. (2019) already included some images collected for this study. Predicted images were post processed through a computer-assisted expert curation using a graphical user interface. Each processed image was assigned a post-processed state, i.e. "correct" or "incorrect", by visually evaluating the predicted image compared to the original one (Bousset *et al.* 2019).

Statistical analyses

We analysed the effects of genotype, year and nitrogen fertilization on stem canker severity using a proportional odds model. We used an ordered logit regression model that handles ordinal data. The design of the experimental data only allowed us to estimate and test the first order effects and the interaction between genotype and nitrogen fertilization.

The density of fruit bodies detected was analysed on the post-processed images validated by the curator (state “correct”). For each image i we considered the number of pixels in states F (fruit bodies) and S (stem), i.e. $n_{F,i}$ and $n_{S,i}$, and used a likelihood function based on $n_{F,i} \sim B[(n_{F,i} + n_{S,i},), p]$ with a logit link function to build Generalised Linear Models and analyse the effects of selected factors with Wald tests. We first considered the complete unbalanced dataset that only enables the identification and test of first order effects (i.e. year, severity prior incubation, plant genotype and nitrogen fertilization) and the interactions between genotype and nitrogen fertilization, and stem severity with nitrogen fertilization (Table 1). Second, in order to go further and investigate second and third order effects (i.e. interactions) we split the 4 years data into 3 datasets: Data14-16 (2 years 14-15 and 15-16, 2 nitrogen fertilization levels Nh and Nl, 15 genotypes), Data12-16 (4 years 12-13, 13-14, 14-15 and 15-16, 15 genotypes, all on high level of fertilization Nh), and Data15-16 (year 15-16, 21 genotypes and 2 nitrogen fertilization levels Nh and Nl). Note that for all these subdatasets the severity prior incubation (7 levels) was also included as a categorical variable in the regression models.

The whole image processing was developed in Python (Van Rossum & Drake 1995) whereas statistical analyses were performed using R (R Core Team 2019).

Prediction of inoculum potential

We simulated the production of inoculum in a population of infected host plants by coupling two stochastic processes. We first considered 10 experimental plots of 100 plants, whose severity drawn from a Multinomial distribution with event probabilities corresponding to those estimated with the ordered logistic regression model (Tables S5.1 and S5.2). Second, we assumed that the size of each individual stem is 700 000 pixels, i.e. twice the average observed number of pixels per processed image, and for each stem we drew the number of fruit body pixels using a Binomial distribution, with probability parameter previously estimated in the GLM model (Tables S5.3 and S5.3). To illustrate the importance of host genotype on fruit body production, we compared the output of the simulation with versus without host genotype.

Results

Severity data at harvest

The observed distribution of canker severities was assessed at harvest, before the sampling of stems selected for fruit body formation assays (See Materials and Methods). Model of the complete ordinal dataset indicated effects (p-values <0.05) of the genotype, the year, the fertilisation and an interaction between genotype and fertilisation on canker severity at harvest (Aggregated G2 index, Table 2; Fig. 2; Fig. S2.1; Fig. S2.2).

Fruit body formation was strongly influenced by year, genotype and disease severity

Across datasets, fruit body formation was affected by host genotype, year, and disease severity at harvest. The year was the most influential parameter, with about 20% of the explained deviance for all analyses (Table 3). Host genotype explained between 6 and 17% of the explained deviance of fruit body formation. Finally, severity of infected stems before incubation explained between 5 and 10 %

of the total deviance. Raw data as well as pairwise comparisons of modalities with least-squares means indicated differences between genotypes and years when stems were collected. The production of fruit bodies was lowest in year 15-16 and highest in year 13-14 (Fig. 3; Supplementary Information S3).

The amount of fruit bodies produced increased with stem canker severity as already shown by Bousset et al. (2019). Stem canker severity classes were ranked from the lowest to highest, except for classes S6 and S5 that were in reversed order (Fig. 4a; Supplementary Information Fig. S3.1; 3.4; 3.7). However, for each severity class, the fruit bodies produced depended on the genotype (Fig. 4; 5; Supplementary Information Fig. S4.1; S4.2). Some genotypes like Al and Fa produced greater numbers of fruit bodies at each severity class than genotypes like As and Av. Noteworthy, here the stem pieces have been individually tracked, so the production of a genotype can be compared at each severity class. One can also note that a severely infected genotype like Yu (having no stem in classes S1 and S2a) is not the one producing the greatest amount of fruit bodies at a given severity class. In contrast, a mildly infected genotype like Da (having no stem in classes S5 and S6) produced more fruit bodies at a given severity class than e.g. genotypes As or Av.

Because several genotypes did not occur either in the first two (S1-S2) or the last two (S5-S6) severity classes, it was not possible to estimate all the coefficients of the genotype × severity interaction on the full dataset. However, when considering the genotypes for which this interaction was identifiable, we found a significant genotype × severity interaction, suggesting that the amount of produced fruit bodies by each severity class may change with host genotypes.

Nitrogen fertilization of the crop has a significant but minor effect on fruit body formation

We detected a significant fertilization × host genotype interaction, indicating that fertilization has varying effects on disease symptoms of different host genotypes. (Fig. 2). The fertilization × disease severity and fertilization × year interactions were also significant. However, as shown by the little deviance explained by these first, second and third order factors, nitrogen fertilization had a

minor influence on fruit body production (Table 3; Fig. 6). In fact, nitrogen explained below 1% of the deviance in the Data15-16 dataset, and only the nitrogen × genotype interaction explained 5% of the deviance (Table 3).

Simulated fruit body formation

The stochastic simulation of fruit body production based on fitted event probabilities (proportional odds and generalized linear models) allowed us to predict the potential level of inoculum produced by field plots for each genotype x year x nitrogen fertilization case (Table S5.1; S5.2; S5.3; S5.4). Simulations outputs illustrate the variability of fruit body formation and confirm the importance of host genotype on this life-history trait of the fungal pathogen (Fig. 7; Fig. S5.1).

When the simulated fruit body production was plotted over canker severity at harvest using the aggregated G2 index, among the genotypes, either susceptible (high canker severity) or with higher levels of quantitative resistance (low canker severity), the pixels of fruit bodies are variable (Fig. 8). A very susceptible genotype is not always the one producing the greatest amount of fruit bodies for the following year. Moreover, genotypes with higher levels of quantitative resistance have low canker severity at harvest but are still diverse with regard to fruit body production (Fig. 8).

Discussion

With field experiments and image-based automated quantification of fruit bodies on individual stems, we disentangled the role of the year, the genotype, the disease severity and the nitrogen fertilization. We confirmed for the first time that the oilseed rape genotype has a direct effect, not only through disease severity, on a seldom-informed trait of the fungal pathogen life cycle. The effect of host genotype on both the visual density of pseudothecia and the numbers of released ascospores had already been observed by Marcroft *et al*. (2004b). However, given the experimental design used, the authors could not clearly distinguish the effect of stem canker severity from the effect of host

genotype. Lô-Pelzer *et al.* (2009) followed by Bousset et al. (2019) detected the effect of host quantitative resistance and field on disease severity and on fruit body production. Yet, those studies were unable to disentangle the role of host genotype, cropping practices as well as the between-season variability. In our study, because all genotypes were planted in the same field and later incubated at the same place, we could exclude confusion with an effect of the environment. Furthermore, as stems were tracked individually, we were able to separate the effect of disease severity from the effect of genotype. One way forward would be assessing canker severity as a quantitative measure for each stem, without losing part of the information into severity classes, for instance by using image-based phenotyping. Then, it would be possible to assess the quantitative relationship between severity and fruit body production among genotypes.

The number of ascospore per pseudothecium ranged from 1000 to 10 000 (Lô-Pelzer *et al*. 2009) and 1000 to 14 000 (Schneider 2005). Estimates were based either on calculating the minimal and maximal volumes of pseudothecia considered as a sphere and asci considered as a spheroid, or on crushing 50 pseurothecia in water with bleach and counting the ascospores with a haemocytometer (Lô-Pelzer *et al*. 2009). Therefore, the numbers of ascospores available for release in cropping areas are huge. Nevertheless, clear gradients of decrease in leaf spot numbers on farmer's oilseed rape fields were observed with increasing distance from emitting spore sources (previous years' oilseed rape fields) (Bousset *et al*. 2015). Further, how far a source would spill ascospores depends on the number of emitted ascospores. This indicates that however large the number of ascospores is, decreasing their number by the means of genotype will contribute to decreasing disease transmission between successive years. In the panel of genotypes considered in the study, the host modulates the production of fruit bodies rather than suppressing it. Therefore, plant genotypes cannot prevent epidemics but may help to mitigate them. As stated later in the discussion, our findings can help identify conditions (i.e. arrangements of cultivars and fields) within a landscape allowing a durable control of the pathogen, which is a current challenge.

Differences in host phenology may contribute to the observed variability among host genotypes. From the biotrophic and asymptomatic presence of the fungus in the stem, visible cankers appear progressively when the crop matures. Moreover, the delay between infection and symptom appearance (i.e. asymptomatic phase) is known to vary between host-plants in a population, and the distribution of the incubation period could also change with some variables like the host-age when the infection occurs (Leclerc *et al*. 2014). When collecting disease data from genotypes differing in phenology, the sampling can occur at different stages in these processes, and thus introduce more variability in the relationship between the visual Phoma stem canker severity and the resulting fruit bodies produced. In oilseed rape stems, pathogen load, i.e. the amount of fungal mycelium, remains low throughout winter and starts to increase as *L. maculans* changes from biotrophic to necrotrophic after host flowering (Gervais *et al*. 2017). Nevertheless, in our study neither the time of flowering nor the time between flowering and harvest appeared as a major determinant of the genotype effect (Table S1.2). A more precise quantification of mycelium, by qPCR or by the visualisation of cankers through non-destructive imaging like MRI, could be helpful to better understand the mechanisms involved in the genotype effect.

Genotype effect could be due to a difference in the amount of nutrients available for the fungus. Indeed, in *P. infestans*, the most severely affected plants during the cropping season were the least prone to the intercrop survival of the pathogen on tubers. As quantitative host resistance reduces disease severity during the cropping season, it thus seems to promote intercrop survival (Pasco *et al*. 2016). However, in our study some genotypes may be severely infected but produce a moderate quantity of fruit bodies (Yu) while others may produce more fruit bodies (Da) than expected based on their Phoma stem canker severity class. Quantitative host resistance does affect inoculum production by decreasing disease severity, as number of pseudothecia on stems increase with Phoma stem canker severity (McGee & Emmett 1977; Marcroft *et al*. 2004a; Lô-Pelzer *et al*. 2009; Bousset *et al*. 2019). In our study, the genotypes Av, Cb, Da, Gr, Jn, Ko had higher than average levels of quantitative resistance on stem canker severity (Table S1.2; Fopa-Fomeju *et al*. 2015; Kumar *et al*.

2018), but they did not show any specific trend regarding fruit body production at a given severity class (Fig. 4; 5). Further, the nitrogen supply affected both disease severity at harvest and fruit body production, though the magnitude of the effect on fruit bodies was relatively small. It could be worth considering this for breeding cultivars for low-input systems. Genetic analyses are needed to identify the determinants underlying fruit body production in the genotypes. So far, plant resistance is still only characterised during the epidemics, e.g. in grapevine (Bove & Rossi 2020). However, pathogen life-cycle stages related to intercrop transmission, like the production of oospores in *Plasmopara viticola,* are starting to be evaluated (Delbac *et al*. 2019). In pathosystems such as downy mildew on grapevine or stem canker on oilseed rape, as host resistance affects pathogen transmission and survival, a low production of fruit bodies could be worth selecting in breeding schemes. At least, discarding the most fruit body-prone genetic backgrounds would be a step forward.

The highlighted effect of host genotype on inoculum carry-over may also be explained by a bias in mating of the fungal pathogen. Because the fungus is heterothallic, mating only occurs when the two mating types are present. A small canker with mycelia of both mating types is thus suitable for mating. In contrast, if a large canker is caused by only one individual, then no pseudothecia could be produced. The occurrence of Allee effects in fungi, i.e. reduced success of mating at low population density, has started to be investigated under controlled conditions for *Zymoseptoria tritici* (Suffert *et al*. 2018b) but should deserve further investigations. In the particular case of *L. maculans*, mycelial growth in the petiole has started to be investigated (Huang *et al*. 2019), but the precise location of the fungus in stem and its consequences on mating remains unknown. Further studies would be interesting and could rely on the use of GFP-transformed strains in controlled conditions or sequencing methods combined with population genetics analyses in natural monitored epidemics.

In agreement with previous findings (Lô-Pelzer *et al*. 2009; Bousset *et al*. 2019), our study confirmed the importance of between-year variability that may be related to variable environmental conditions. The highest fruit bodies numbers (Fig. 2) and rainfall during incubation (Fig. S1d) were

362 observed in year 13-14. In contrast, the lowest fruit bodies numbers and rainfall during incubation
363 were observed in year 15-16. While the effects of climatic variables on maturation of the fruit bodies
364 have been modelled (Aubertot *et al*. 2006), their influences on the pathogen during the cropping
365 season and during the intercrop still deserve further investigations. In particular, besides influencing
366 the development of the host plant, some main climatic variables such as temperature may drive
367 within-host pathogen growth, influence pathogen load at stem base, thus influence mating of the
368 fungus and therefore fruit body production. Linking environmental conditions with host and pathogen
369 development is a current challenge for most pathosystems to improve predictions of epidemics and
370 yields. In the particular case of oilseed rape stem canker, further studies are needed to address the
371 influence of crop growth in real situations as well as intercrop practices of the production of fruit
372 bodies (McCredden *et al*. 2017).

373 As plant genotype appeared to be an important driver of the production of inoculum, this
374 should be taken into account in models used to compare strategies for the deployment of varieties in
375 the landscape (Lô-Pelzer *et al*. 2010; Papaïx *et al*. 2018; Rimbaud *et al*. 2018; Watkinson-Powell *et*
376 *al*. 2019). So far, the effect of qualitative host resistance on infection and some effects of quantitative
377 host resistance on pathogen development are considered. Our results suggest that it would be worth
378 considering the effect of host quantitative resistance on the pathogen during the intercrop. One
379 striking result of our stochastic simulations of fruit body production is that the ranking of the
380 genotypes (Fig. 7) appeared to be very different from the ranking obtained when considering the
381 disease severity at harvest (Fig. 2). For example, the genotypes Ja, Pr and Yu with a high disease
382 severity at harvest (Fig.2) produce fewer fruit bodies than others (Fig.7). In contrast, the genotypes
383 Fa, Fr and Po have a moderate disease severity at harvest (Fig.2) but later produce higher amounts of
384 fruit bodies that others (Fig.7). Recognition of this trade-off in pathogen resistance properties may
385 help breeding varieties less prone to inoculum production and guide further breeding schemes.
386

387 **Acknowledgements**

We thank UE La Motte for running the cultivation of the experiments. We thank Yannick Lucas, Claude Domin and casual workers for technical assistance. We thank BraCySol biological resource centre (INRA Ploudaniel, France) for providing the seeds used in this study. We are grateful to the INRA CLIMATIK database for the weather data. This work benefited from the financial support of INRA - the French National Institute for Agronomical Research, and from ANR - the French National Research Agency – program AGROBIOSPHERE grant ANR-11-AGRO-003-01 and from the French Association for the Promotion of Oilseed Crops Breeding (PROMOSOL) through the project MOREAZ (Modulation de la réponse de résistance du colza à des agents pathogènes (hernie et phoma) en situation de contrainte azotée).

Authors' contributions

LB, PV and RD carried out experiments, ML carried out statistical analyses, LB, ML, NP and MP analysed pictures. LB conceived and designed the study and prepared the manuscript, read and approved by all authors. The authors declare the absence of conflict of interest.

References

Aubertot J, Salam MU, Diggle AJ, Dakowska S, Jedryczka M, 2006. Simmat, a new dynamic module of blackleg sporacle for the prediction of pseudothecia maturation of *L. maculans*/*L. biglobosa* species complex parameterisation and evaluation in Polish conditions. *IOBC WPRS Bulletin* **29**: 277-285.

Bailey D, Kleczkowski A, Gilligan C, 2004. Epidemiological dynamics and the efficiency of biological control of soil-borne disease during consecutive epidemics in a controlled environment. *New Phytologist* **161**: 569–575.

Bouchet A, Nesi N, Bissuel C, Bregeon M, Lariepe A, Navier H, Ribière N, Orsel M, Grezes-Besset B, Renard M, Laperche A, 2014. Genetic control of yield and yield components in winter oilseed rape (*Brassica napus* L.) grown under nitrogen limitation. *Euphytica* **199**: 183–205.

Bousset L, Palerme M, Leclerc M, Parisey N, 2019. Automated image processing framework for analysis of the density of fruiting bodies of *Leptosphaeria maculans* on oilseed rape stems. *Plant Pathology* **68**: 1749–1760.

Bousset L, Chèvre AM, 2013. Stable epidemic control in crops based on evolutionary principles: adjusting the metapopulation concept to agro-ecosystems. *Agriculture, Ecosystems and Environment* **165**: 118–129.

Bousset L, Jumel S, Garreta V, Picault H, Soubeyrand S, 2015. Transmission of *Leptosphaeria maculans* from a cropping season to the following one. *Annals of Applied Biology* **166**: 530–543.

Bousset L, Sprague SJ, Thrall PH, Barrett LG, 2018. Spatio-temporal connectivity and host resistance influence evolutionary and epidemiological dynamics of the canola pathogen *Leptosphaeria maculans*. *Evolutionary Applications* **11**: 1354–1370.

Bove F, Rossi V, 2020. Components of partial resistance to *Plasmopara viticola* enable complete phenotypic characterization of grapevine varieties. *Scientific Reports* **10**: 585.

Brun H, Chèvre AM, Fitt BDL, Powers S, Besnard AL, Ermel M, Huteau V, Marquer B, Eber F, Renard M, Andrivon D, 2010. Quantitative resistance increases the durability of qualitative resistance to *Leptosphaeria maculans* in *Brassica napus*. *New Phytologist* **185**: 285–299.

Bruns E, Carson M, May G, 2012. Pathogen and host genotype differently affect pathogen fitness through their effects on different life-history stages. *BMC Evolutionary Biology* **12**: 135.

Burdon JJ, Zhan J, Barrett LG, Papaïx J, Thrall PH, 2016. Addressing the challenges of pathogen evolution on the world's arable crops. *Phytopathology* **106**: 1117–1127.

Cowger C, Brown JKM, 2019. Durability of quantitative resistance in crops: greater than we know? *Annual Review of Phytopathology* **57**: 253–77.

440 Daverdin G, Rouxel T, Gout L, Aubertot JN, Fudal I, Meyer M, Parlange F, Carpezat J, Balesdent
441 MH, 2012. Genome structure and reproductive behaviour influence the evolutionary potential
442 of a fungal phytopathogen. *PLoS Pathogens* **8**: e1003020.
443 Delbac L, Delière L, Schneider C, Delmotte F, 2019. Evidence for sexual reproduction and fertile
444 oospore production by *Plasmopara viticola* on the leaves of partially resistant grapevine
445 cultivars. *Acta Horticulturae* **1248**: 607–620.
446 Delmas CEL, Fabre F, Jolivet J, Mazet ID, Cervera SR, Delière L, Delmotte F, 2016. Adaptation of a
447 plant pathogen to partial host resistance: selection for greater aggressiveness in grapevine
448 downy mildew. *Evolutionary Applications* **9**: 709–725.
449 Delourme R, Bousset L, Ermel E, Duffé P, Besnard AL, Marquer B, Fudal I, Linglin J, Chadœuf J,
450 Brun H, 2014. Quantitative resistance affects the speed of frequency increase but not the
451 diversity of the virulence alleles overcoming a major resistance gene to *Leptosphaeria*
452 *maculans* in oilseed rape. *Infection, Genetics & Evolution* **27**: 490–499.
453 Didelot F, Caffier V, Orain G, Lemarquand A, Parisi L, 2016. Sustainable management of scab control
454 through the integration of apple resistant cultivars in a low-fungicide input system.
455 *Agriculture, Ecosystems & Environment* **217**: 41–48.
456 Dumartinet T, Abadie C, Bonnot F, Carreel F, Roussel V, Habas R, Martinez RT, Perez-Vicente L,
457 Carlier J, 2020. Pattern of local adaptation to quantitative host resistance in a major pathogen
458 of a perennial crop. *Evolutionary Applications* **13**: 824–836.
459 Fopa Fomeju B, Falentin C, Lassalle G, Manzanares-Dauleux M, Delourme R, 2015. Comparative
460 genomic analysis of duplicated homoeologous regions involved in the resistance of *Brassica*
461 *napus* to stem canker. *Frontiers in Plant Science* **6**: 772.
462 Gervais J, Plissonneau C, Linglin J, Meyer M, Labadie K, Cruaud C, Fudal I, Rouxel T, Balesdent
463 MH, 2016. Different waves of effector genes with contrasted genomic location are expressed
464 by *Leptosphaeria maculans* during cotyledon and stem colonisation of oilseed rape.
465 *Molecular Plant Pathology* **18**: 1113–1126.

Huang YJ, Paillard S, Kumar V, King GJ, Fitt BDL, Delourme R, 2019. Oilseed rape (*Brassica napus*) resistance to growth of *Leptosphaeria maculans* in leaves of young plants contributes to quantitative resistance in stems of adult plants. *PLoS ONE* **14**(9): e0222540.

Karisto P, Hund A, Yu K, Anderegg J, Walter A, Mascher F, McDonald BA, Mikaberidze A, 2018. Ranking quantitative resistance to *Septoria tritici* blotch in elite wheat cultivars using automated image analysis. *Phytopathology* **108**: 568–581.

Kumar V, Paillard S, Fopa-Fomeju B, Falentin C, Deniot G, Baron C, Vallée P, Manzanares-Dauleux M, Delourme R, 2018. Multi-year linkage and association mapping confirm the high number of genomic regions involved in oilseed rape quantitative resistance to blackleg. *Theoretical and Applied Genetics* **131**: 1627–1643.

Lasserre-Zuber P, Caffier V, Stievenard R, Lemarquand A, Le Cam B, Durel CE, 2018. Pyramiding quantitative resistance with a major resistance gene in apple: from ephemeral to enduring effectiveness in controlling scab. *Plant Disease* **102**: 2220–2223.

Leclerc M, Clément JAJ, Andrivon D, Hamelin FM, 2019. Assessing the effects of quantitative host resistance on the life-history traits of sporulating parasites with growing lesions. *Proceedings of the Royal Society B: Biological Sciences* **286**: (1912), 20191244.

Leclerc M, Doré T, Gilligan CA, Lucas P, Jan F, 2014. Estimating the delay between host infection and disease (incubation period) and assessing its significance to the epidemiology of plant diseases. *PLoS ONE* **9**: 1–15.

Lô-Pelzer E, Aubertot JN, David O, Jeuffroy MH, Bousset L, 2009. Relationship between severity of blackleg (*Leptosphaeria maculans*/*L.biglobosa* species complex) and subsequent primary inoculum production on oilseed rape stubble. *Plant Pathology* **58**: 61–70.

Lô-Pelzer E, Bousset L, Jeuffroy MH, Salam MU, Pinochet X, Boillot M, Aubertot JN, 2010. SIPPOM-WOSR : A simulator for integrated pathogen population management of phoma stem canker on winter oilseed rape. I. Description of the model. *Field Crops Research* **118**: 73–81.

492 Marcroft S, Sprague S, Salisbury P, Howlett B, 2004b. Potential for using host resistance to reduce
493 production of pseudothecia and ascospores of *Leptosphaeria maculans*, the blackleg pathogen
494 of *Brassica napus*. *Plant Pathology* **53**: 468–474.
495 Marcroft SJ, Sprague SJ, Pymer SJ, Salisbury PA, Howlett BJ, 2004a. Crop isolation, not extended
496 rotation length, reduces blackleg (*Leptosphaeria maculans*) severity of canola (*Brassica*
497 *napus*) in south-eastern Australia. *Australian Journal of Experimental Agriculture* **44**: 601–
498 606.
499 McCredden J, Cowley RB, Marcroft SJ, Van de Wouw AP, 2017. Changes in farming practices impact
500 on spore release patterns of the blackleg pathogen, *Leptosphaeria maculans*. *Crop and Pasture*
501 *Science* **69**: 1–8.
502 McGee D, Emmett R, 1977. Blackleg (*Leptosphaeria maculans* (desm.) ces. et de not.) of rapeseed
503 in Victoria: crop losses and factors which affect disease severity. *Australian Journal of*
504 *Agricultural Research* **28**: 47–51.
505 Papaïx J, Rimbaud L, Burdon JJ, Zhan J, Thrall PH, 2018. Differential impact of landscape-scale
506 strategies for crop cultivar deployment on disease dynamics, resistance durability and long-
507 term evolutionary control. *Evolutionary Applications* **11**: 705–717.
508 Pasco C, Montarry J, Marquer B, Andrivon D, 2016. And the nasty ones lose in the end: foliar
509 pathogenicity trades off with asexual transmission in the Irish famine pathogen *Phytophthora*
510 *infestans*. *New Phytologist* **209**: 334–342.
511 R Core Team (2020). R: A language and environment for statistical computing. R Foundation for
512 Statistical Computing, Vienna, Austria. URL https://www.R-project.org/.
513 Rimbaud L, Papaïx J, Rey JF, Barrett LG, Thrall PH, 2018. Assessing the durability and efficiency of
514 landscape-based strategies to deploy plant resistance to pathogens. *PLoS Computational*
515 *Biology* 14(4): e1006067.

516 Schneider O, 2005. Analyse du Mode de Gestion des Résidus de Colza sur l'Initiation du Cycle de
517 *Leptosphaeria maculans* (Desm.) Ces et de Not. INRA Centre de Versailles-Grignon, France:
518 INA PG, PhD thesis.
519 Stewart EL, Hagerty CH, Mikaberidze A, Mundt CC, Zhong Z, McDonald BA, 2016. An improved
520 method for measuring quantitative resistance to the wheat pathogen *Zymoseptoria tritici* using
521 high-throughput automated image analysis. *Phytopathology* **106**: 782–788.
522 Suffert F, Goyeau H, Sache I, Carpentier F, Gélisse S, Morais D, Delestre G, 2018a. Epidemiological
523 trade-off between intra- and interannual scales in the evolution of aggressiveness in a local
524 plant pathogen population. *Evolutionary Applications* **11**: 768–780.
525 Suffert F, Delestre G, Gélisse S, 2018b. Sexual reproduction in the fungal foliar pathogen
526 *Zymoseptoria tritici* is driven by antagonistic density-dependence mechanisms. *Microbial*
527 *Ecology* **77**: 110–23.
528 Van Rossum G, Drake Jr FL, 1995. Python reference manual. Centrum voor Wiskunde en Informatica
529 Amsterdam.
530 Watkinson-Powell B, Gilligan CA, Cunniffe NJ, 2019. When does spatial diversification usefully
531 maximise the durability of crop disease resistance? *Phytopathology*. Online Doi:
532 10.1094/PHYTO-07-19-0261-R
533 West JS, Kharbanda P, Barbetti M, Fitt BDL, 2001. Epidemiology and management of *Leptosphaeria*
534 *maculans* (phoma stem canker) on oilseed rape in Australia, Canada and Europe. *Plant*
535 *Pathology* **50**: 10–27.
536 Wherrett A, Sivasithamparam K, Barbetti M, 2003. Chemical manipulation of *Leptosphaeria*
537 *maculans* (blackleg disease) pseudothecial development and timing of ascospore discharge
538 from canola (*Brassica napus*) residues. *Australian Journal of Agricultural Research* **54**: 837–
539 848.
540 Yang X, Hong C, 2018. Microsclerotial enumeration, size, and survival of *Calonectria*
541 *pseudonaviculata*. *Plant Disease* **102**: 983–990.

Zadoks JC, Schein RD, 1979. *Epidemiology and Plant Disease Management*, Oxford University Press, New York, NY, USA.

Zhan J, Thrall PH, Papaïx J, Xie L, Burdon JJ, 2015. Playing on a pathogen's weakness: Using evolution to guide sustainable plant disease control strategies. *Annual Review of Phytopathology* **53**: 19–43.

Figure Legends

Fig. 1. Schematic representation of cyclic epidemics and their control by plant resistance. (**A**) Cyclic epidemics are characterized over years by the disease being present in the landscape with a stable long term dynamics (black dashed line), but short term dynamics alternating between epidemic phase (red lines) when the crop is present and decrease (blue lines) during the intercrop (Ic.). (**B**) Plant genetic resistance can contribute to the control of cyclic epidemics during the crop with qualitative resistance reducing infection and quantitative resistance reducing the increase. During the intercrop, the selective deployment of genotypes reduces landscape connectivity, and the plant genotype influence the amount of inoculum produced (this study).

Fig. 2. Canker severity (G2 index) on field plots depending on the nitrogen level and the genotype. The model was adjusted to the data of 12-13 to 15-16 years. Full names of genotypes and flowering dates are available (Supplementary Information Table S1.2).

Fig. 3. Fraction of fruit body pixels depending on year of sampling (12-13, 13-14, 14-15 and 15-16) for the fifteen genotypes in the Data12-16 dataset. Full names of genotypes are available (Supplementary Information Table S1.2).

Fig. 4. Fraction of fruit body pixels depending for the S1 to S6 severity classes in the Data14-16 dataset. (A) For all genotypes; (B) to (H) per genotype for each of the six severity classes. Full names of genotypes are available (Supplementary Information Table S1.2).

Fig. 5. Fraction of fruit body pixels depending on the severity before incubation exemplified for the fifteen genotypes in the Data14-16 dataset. This result was observed for all datasets (Supplementary Information Fig. S4.1; S4.2). Full names of genotypes are available (Supplementary Information Table S1.2).

Fig. 6. Predicted fraction of fruit body pixels depending on the twenty one genotypes in the Data15-16 dataset for (A) normal (Nh) or (B) reduced (Nl) nitrogen fertilization of the crop. Full names of genotypes are available (Supplementary Information Table S1.2).

Fig. 7 Boxplot of simulated numbers of fruit body pixels depending on the normal (Nh) or reduced (Nl) nitrogen level and on the genotype (21 genotypes). The effect of genotype was taken into account both for the distribution of stems in canker severity classes and on the prediction of fruit body pixels, adjusting the model on observed data. Overall are values without the genotype effect. Data are means of 10 simulated field plots with 100 plants of 700 000 pixels. Full names of genotypes are available (Supplementary Information Table S1.2).

Fig. 8 Average simulated numbers of fruit body pixels depending on the canker severity at harvest (G2 index calculated for the ensemble of stems) for the fifteen genotypes over all years. In simulations, the effect of genotype was taken into account both for the distribution of stems in canker severity classes and on the prediction of fruit body pixels, adjusting the model on observed data. Data are means of 10 simulated field plots with 100 plants of 700 000 pixels. Among the genotypes, either susceptible (high canker severity) or with higher levels of quantitative resistance (low canker

593 severity), the pixels of fruit bodies are variable. A very susceptible genotype (Yu) is not the one
594 leaving the greatest amount of fruit bodies.
595
596

Fig 1

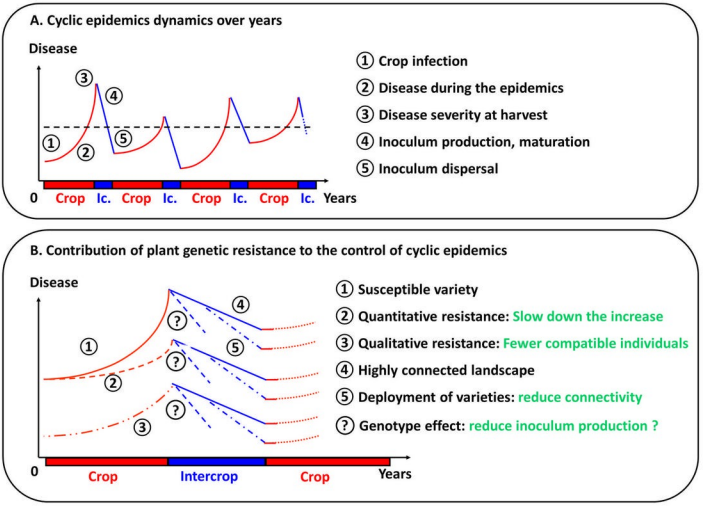
A. Cyclic epidemics dynamics over years
Disease
0
Crop
Ic.
Crop
Ic.
Crop
Ic.
Crop
Ic.
Years
① Crop infection
② Disease during the epidemics
③ Disease severity at harvest
④ Inoculum production, maturation
⑤ Inoculum dispersal
B. Contribution of plant genetic resistance to the control of cyclic epidemics
Disease
0
Crop
Intercrop
Crop
Years
① Susceptible variety
② Quantitative resistance: Slow down the increase
③ Qualitative resistance: Fewer compatible individuals
④ Highly connected landscape
⑤ Deployment of varieties: reduce connectivity
? Genotype effect: reduce inoculum production ?

Fig 2

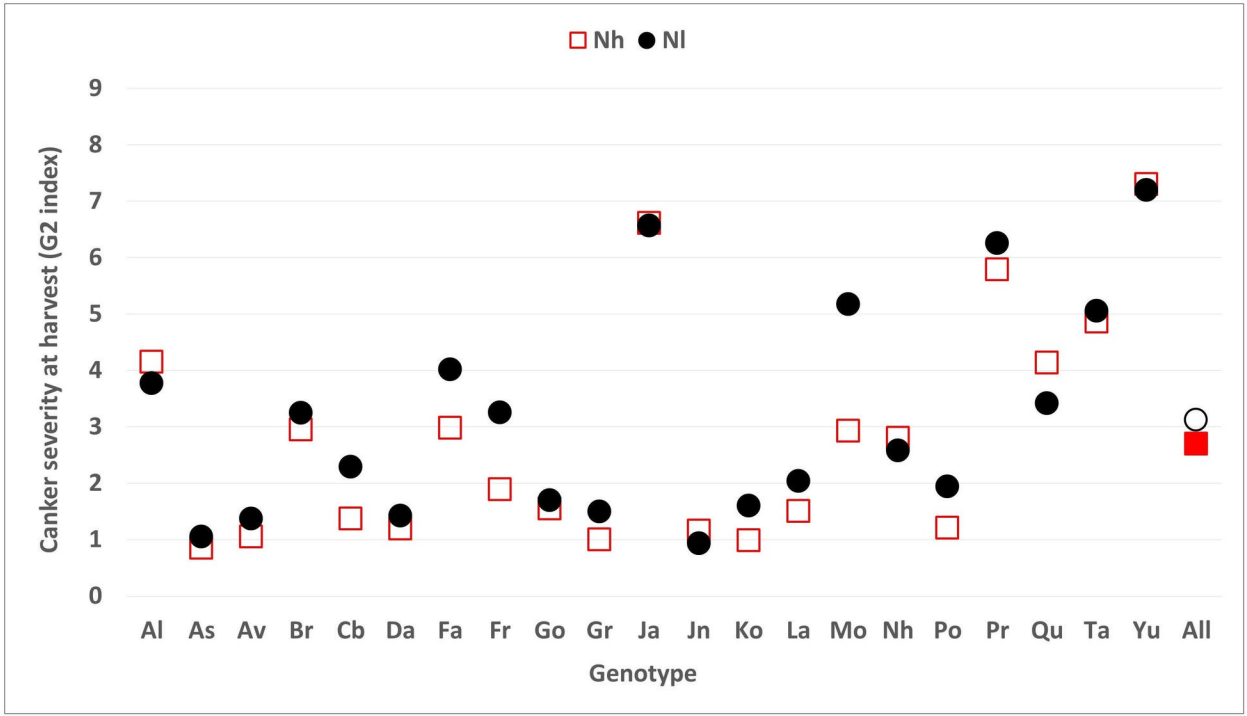
Nh
Nl
Canker severity at harvest (G2 index)
0
1
2
3
4
5
6
7
8
9
Al
As
Av
Br
Cb
Da
Fa
Fr
Go
Gr
Ja
Jn
Ko
La
Mo
Nh
Po
Pr
Qu
Ta
Yu
All
Genotype

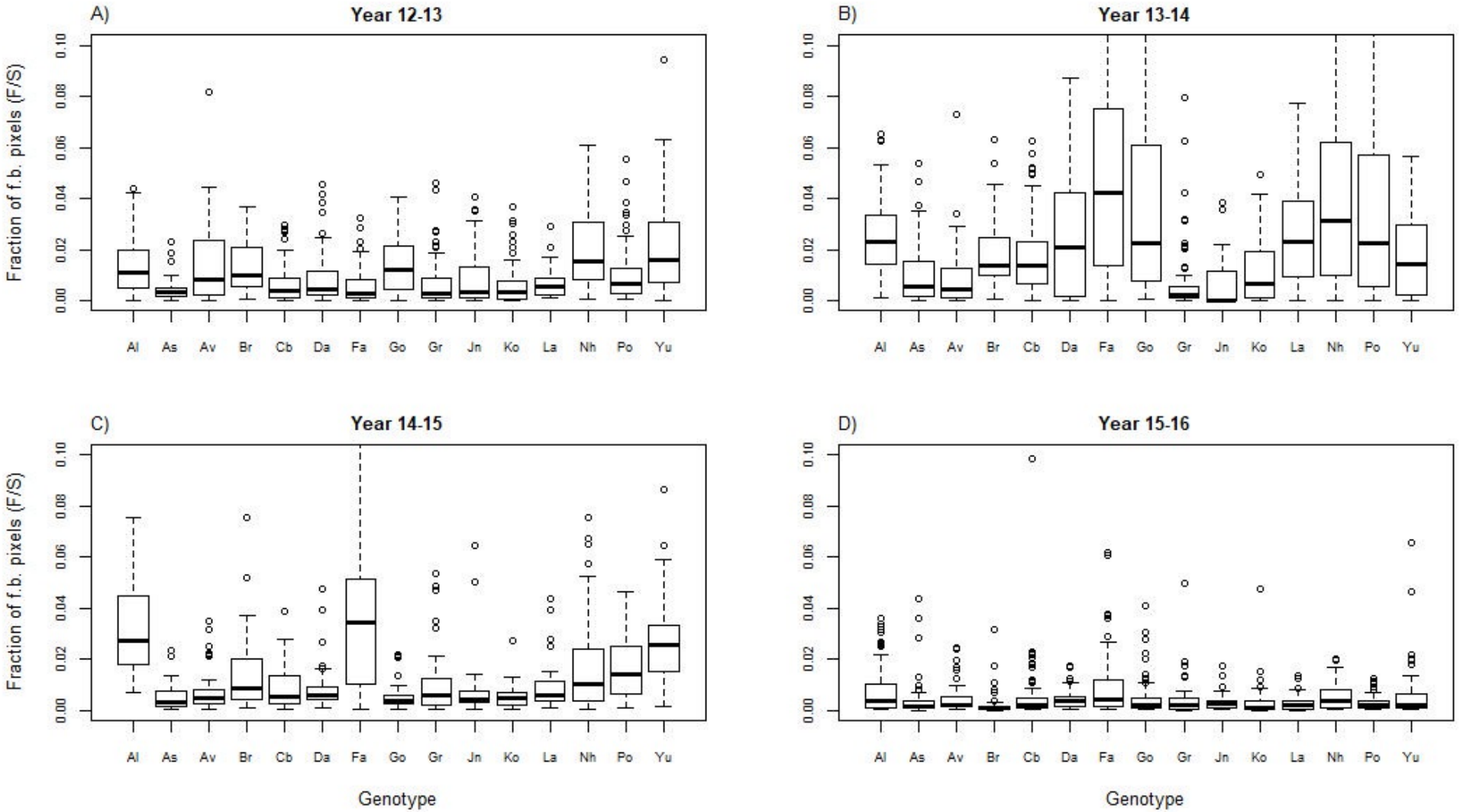
A)
Year 12-13
B)
Year 13-14
C)
Year 14-15
D)
Year 15-16
Fraction of f.b. pixels (F/S)
0.00
0.02
0.04
0.06
0.08
0.10
Al
As
Av
Br
Cb
Da
Fa
Go
Gr
Jn
Ko
La
Nh
Po
Yu
Genotype

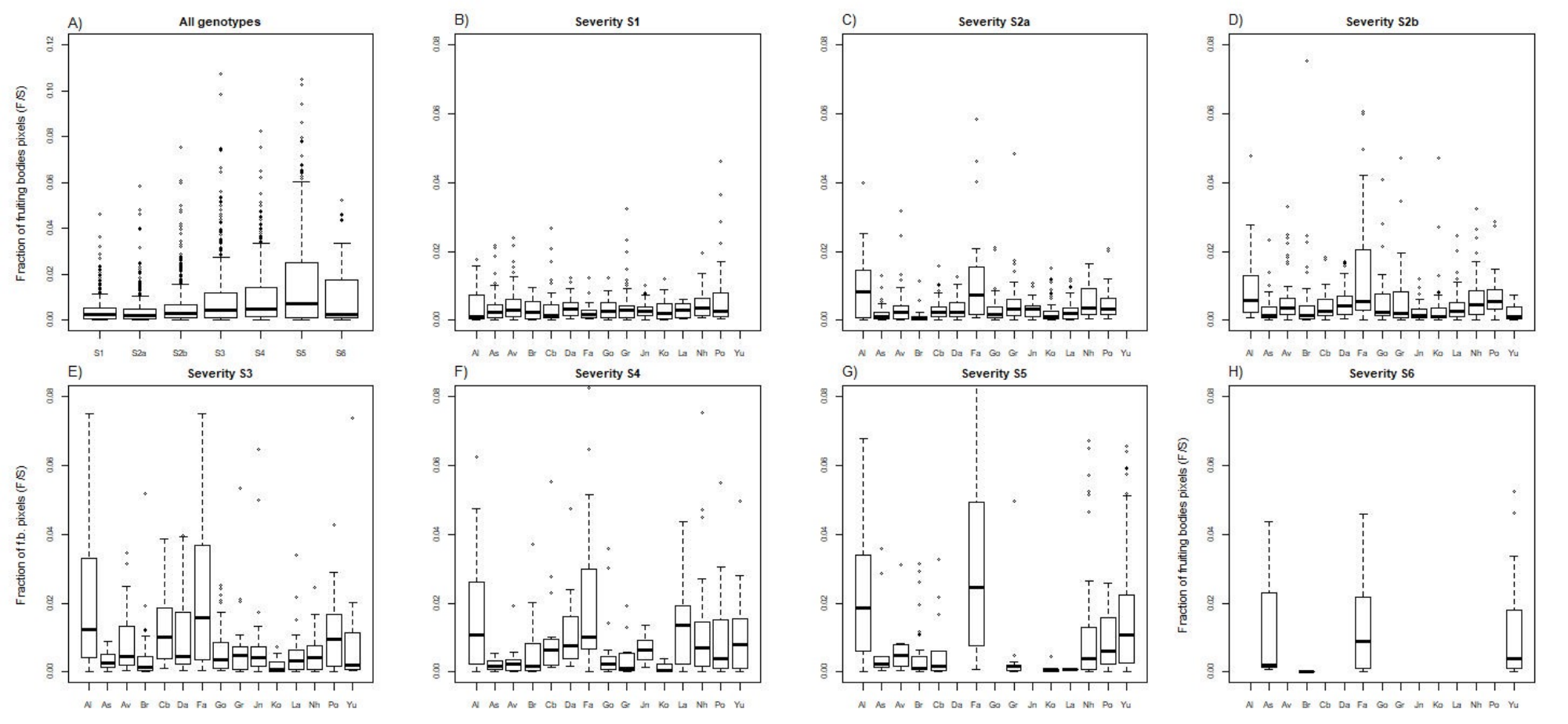
A)
All genotypes
B)
Severity S1
C)
Severity S2a
D)
Severity S2b
E)
Severity S3
F)
Severity S4
G)
Severity S5
H)
Severity S6
Fraction of fruiting bodies pixels (F/S)
Fraction of f.b. pixels (F/S)
S1 S2a S2b S3 S4 S5 S6
Al As Av Br Cb Da Fa Go Gr Jn Ko La Nh Po Yu

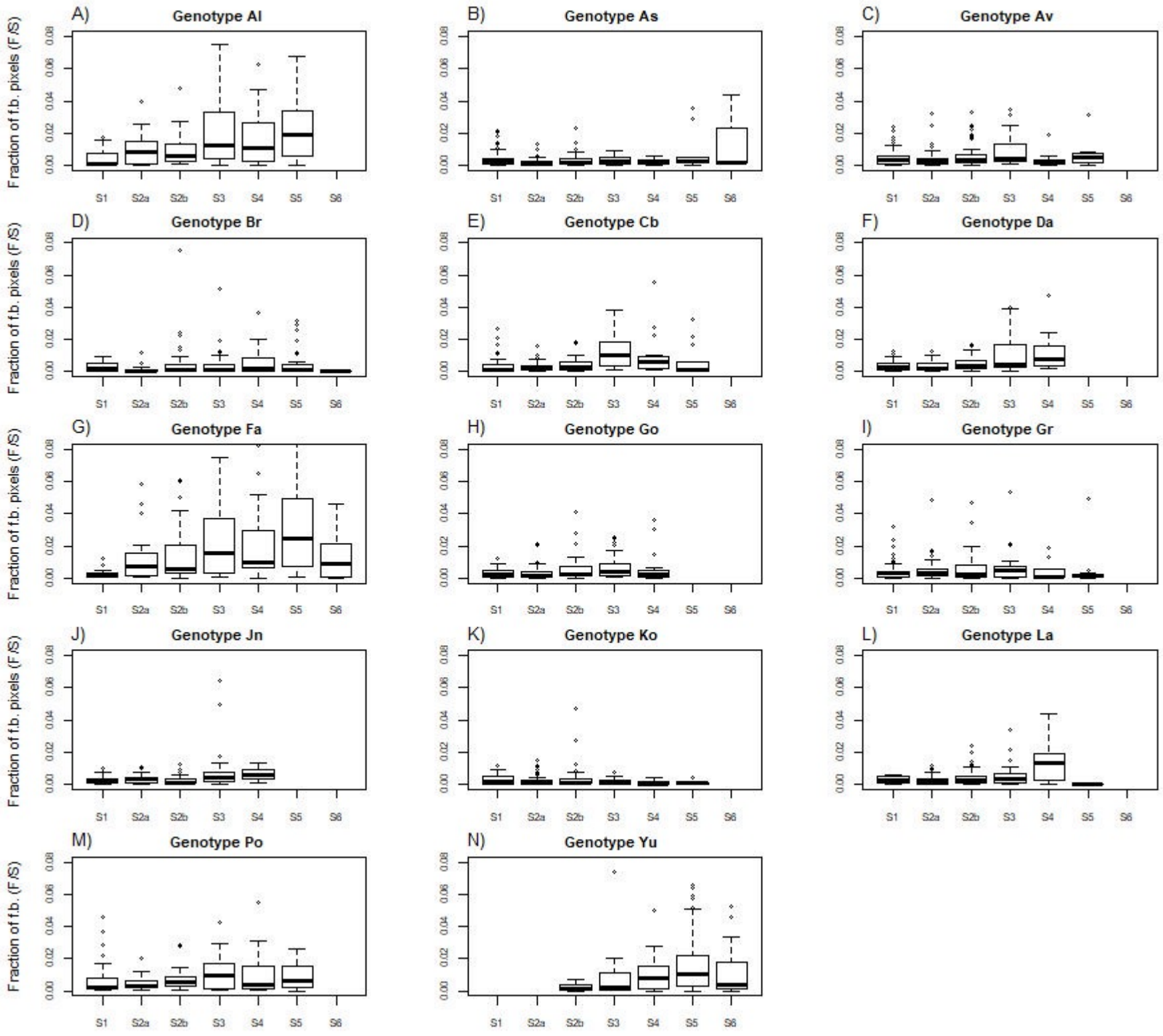
A)
Genotype Al
B)
Genotype As
C)
Genotype Av
D)
Genotype Br
E)
Genotype Cb
F)
Genotype Da
G)
Genotype Fa
H)
Genotype Go
I)
Genotype Gr
J)
Genotype Jn
K)
Genotype Ko
L)
Genotype La
M)
Genotype Po
N)
Genotype Yu
Fraction of f.b. pixels (F/S)
Fraction of f.b. (F/S)
0.00
0.02
0.04
0.06
0.08
S1
S2a
S2b
S3
S4
S5
S6

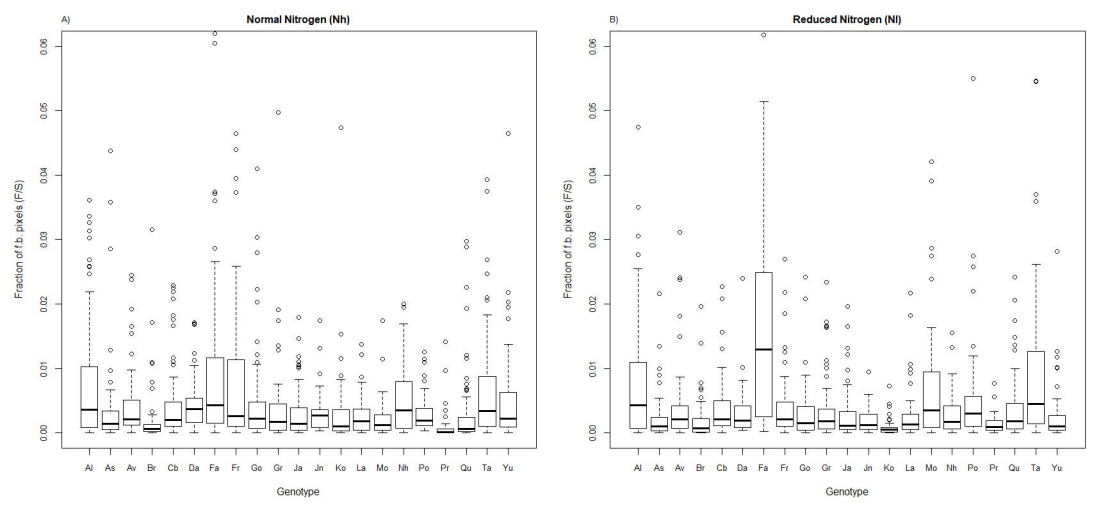
A)
Normal Nitrogen (Nh)
Fraction of f.b. pixels (F/S)
0.00
0.01
0.02
0.03
0.04
0.05
0.06
Al As Av Br Cb Da Fa Fr Go Gr Ja Jn Ko La Mo Nh Po Pr Qu Ta Yu
Genotype
B)
Reduced Nitrogen (Nl)
Fraction of f.b. pixels (F/S)
0.00
0.01
0.02
0.03
0.04
0.05
0.06
Al As Av Br Cb Da Fa Fr Go Gr Ja Jn Ko La Mo Nh Po Pr Qu Ta Yu
Genotype

Fig 7

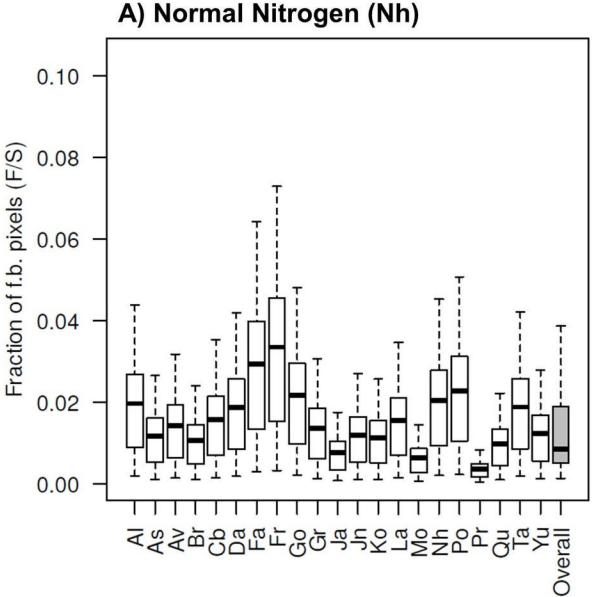
A) Normal Nitrogen (Nh)
Fraction of f.b. pixels (F/S)
0.10
0.08
0.06
0.04
0.02
0.00
Al
As
Av
Br
Cb
Da
Fa
Fr
Go
Gr
Ja
Jn
Ko
La
Mo
Nh
Po
Pr
Qu
Ta
Yu
Overall

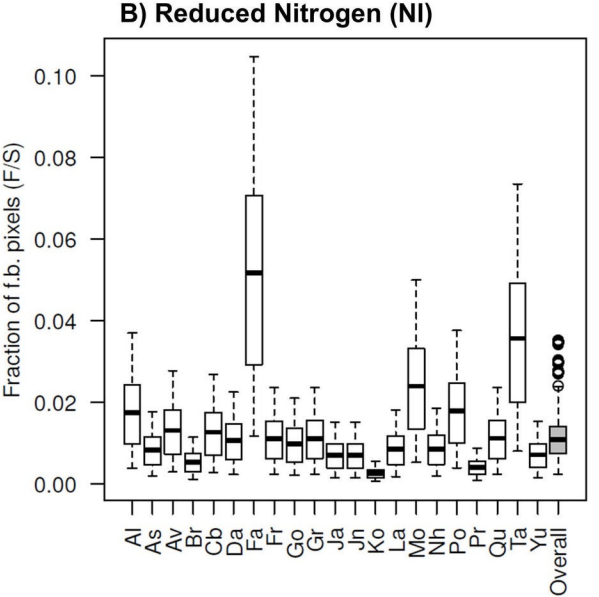
B) Reduced Nitrogen (Nl)
Fraction of f.b. pixels (F/S)
0.10
0.08
0.06
0.04
0.02
0.00
Al
As
Av
Br
Cb
Da
Fa
Fr
Go
Gr
Ja
Jn
Ko
La
Mo
Nh
Po
Pr
Qu
Ta
Yu
Overall

Fig 8

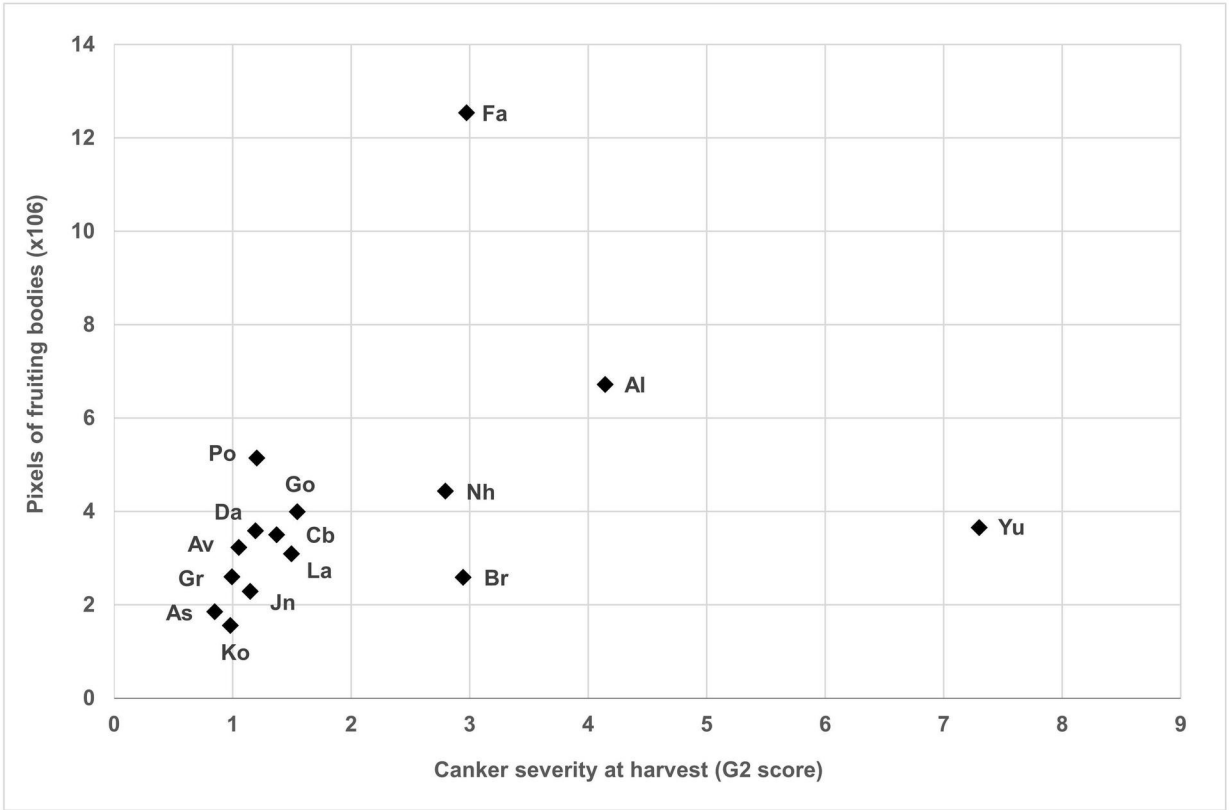
Pixels of fruiting bodies (x106)
Canker severity at harvest (G2 score)
0
2
4
6
8
10
12
14
0
1
2
3
4
5
6
7
8
9
Fa
Al
Po
Go
Nh
Da
Cb
Yu
Av
La
Br
Gr
Jn
As
Ko

Table 1. Numbers of stems for the complete and the three sub datasets (Data14-16, Data12-16, Data15-16) given overall (italicised), but also by year and nitrogen fertilization treatment (Nl and Nh) and by genotype.

Dataset	Year	Nitrogen	Post process			Genotype																				
			Before	Discard	After	Al	As	Av	Br	Cb	Da	Fa	Go	Gr	Jn	Ko	La	Nh	Po	Yu	Fr	Ja	Mo	Pr	Qu	Ta
Complete	**All**		**6758**	**18.3%**	**5525**	**390**	**318**	**366**	**325**	**356**	**286**	**338**	**290**	**348**	**247**	**291**	**320**	**363**	**291**	**273**	**114**	**133**	**137**	**76**	**181**	**82**
	12-13	Nh	938	36	*902*	96	50	70	58	67	64	56	49	54	60	58	44	77	60	39	-	-	-	-	-	-
	13-14	Nh	919	48	*871*	49	59	75	52	88	48	73	42	65	12	31	80	86	70	41	-	-	-	-	-	-
	14-15	Nh	826	222	*604*	72	41	37	15	37	40	57	40	40	43	27	29	57	35	34	-	-	-	-	-	-
	14-15	Nl	789	318	*471*	38	31	30	47	23	25	39	23	32	24	27	36	24	23	49	-	-	-	-	-	-
	15-16	Nh	1626	240	*1386*	67	78	77	77	73	57	61	66	71	44	78	71	76	47	59	48	68	91	35	96	46
	15-16	Nl	1660	369	*1291*	68	59	77	76	68	52	52	70	86	64	70	60	43	56	51	66	65	46	41	85	36
Data1416	**All**		**4045**	**10.1%**	**3029**	**245**	**209**	**221**	**215**	**201**	**174**	**209**	**199**	**229**	**175**	**202**	**196**	**200**	**161**	**193**	**-**	**-**	**-**	**-**	**-**	**-**
	14-15	Nh	826	222	*604*	72	41	37	15	37	40	57	40	40	43	27	29	57	35	34	-	-	-	-	-	-
	14-15	Nl	789	318	*471*	38	31	30	47	23	25	39	23	32	24	27	36	24	23	49	-	-	-	-	-	-
	15-16	Nh	1208	206	*1002*	67	78	77	77	73	57	61	66	71	44	78	71	76	47	59	-	-	-	-	-	-
	15-16	Nl	1222	270	*952*	68	59	77	76	68	52	52	70	86	64	70	60	43	56	51	-	-	-	-	-	-
Data1216	**All**		**3685**	**3.1%**	**3379**	**284**	**228**	**259**	**202**	**265**	**209**	**247**	**197**	**230**	**159**	**194**	**224**	**296**	**212**	**173**	**-**	**-**	**-**	**-**	**-**	**-**
	12-13	Nh	938	36	*902*	96	50	70	58	67	64	56	49	54	60	58	44	77	60	39	-	-	-	-	-	-
	13-14	Nh	919	48	*871*	49	59	75	52	88	48	73	42	65	12	31	80	86	70	41	-	-	-	-	-	-
	14-15	Nh	826	222	*604*	72	41	37	15	37	40	57	40	40	43	27	29	57	35	34	-	-	-	-	-	-
	15-16	Nh	1002	206	*1002*	67	78	77	77	73	57	61	66	71	44	78	71	76	47	59	-	-	-	-	-	-
Data1516	**All**		**3286**	**6.1%**	**2677**	**135**	**137**	**154**	**153**	**141**	**109**	**113**	**136**	**157**	**108**	**148**	**131**	**119**	**103**	**110**	**114**	**133**	**137**	**76**	**181**	**82**
	15-16	Nh	1626	240	*1386*	67	78	77	77	73	57	61	66	71	44	78	71	76	47	59	48	68	91	35	96	46
	15-16	Nl	1660	369	*1291*	68	59	77	76	68	52	52	70	86	64	70	60	43	56	51	66	65	46	41	85	36

Table 2. Analysis of deviance for the observed distribution of canker severities at harvest

Factor	**Df**	**$\chi 2$**	**P-value**
Year	3	7742	< 2.2e-16
Nitrogen	1	211	< 2.2e-16
Genotype	20	8828	< 2.2e-16
Nitrogen × Genotype	20	1971	< 2.2e-16

Table 3: Analysis of deviance for the three datasets, with percentage of deviance explained by each factor and by the model

Dataset	Analysis of deviance				Model
	Factor	**Df**	**P-value**	**Explained deviance**	**R^2**
All	Year	3	<0.05	0.20	0.34
	Genotype	20	<0.05	0.061	
	Severity	6	<0.05	0.069	
	Nitrogen	1	<0.05	<0.001	
	Nitrogen × Genotype	20	<0.05	0.014	
	Nitrogen × Severity	6	<0.05	<0.001	
Data14-16	Nitrogen	1	<0.05	0.01	0.51
	Year	1	<0.05	0.20	
	Genotype	14	<0.05	0.17	
	Severity	6	<0.05	0.08	
	Nitrogen × Year	1	<0.05	0.0002	
	Nitrogen × Genotype	14	<0.05	0.003	
	Year × Genotype	14	<0.05	0.01	
	Year × Severity	6	<0.05	0.01	
	Nitrogen × Severity	6	<0.05	0.01	
	Nitrogen × Year × Genotype	14	<0.05	0.02	
	Nitrogen × Year × Severity	6	<0.05	0.002	
Data12-16	Year	3	<0.05	0.235	0.52
	Genotype	14	<0.05	0.115	
	Severity	6	<0.05	0.096	
	Year × Genotype	42	<0.05	0.062	
	Year × Severity	18	<0.05	0.011	
Data15-16	Nitrogen	1	<0.05	0.0003	0.28
	Genotype	20	<0.05	0.17	
	Severity	6	<0.05	0.05	
	Nitrogen × Genotype	20	<0.05	0.05	
	Nitrogen × Severity	6	<0.05	0.009	